SATELLITE-BASED TROPICAL WARM POOL SURFACE HEAT BUDGETS: CONTRASTS BETWEEN 1997-98 EL NINO AND 1998-99 LA NINA

Shu-Hsien Chou, Ming-Dah Chou, and Po-Hsiung Lin
National Taiwan University, Taipei, Taiwan

Pui-King Chan
Science System & Applications Ins., Maryland, USA

Kung-Hwa Wang
Central Weather Bureau, Taipei, Taiwan

Abstract

The 1997-98 is a strong El Nino warm event, while the 1998-99 is a moderate La Nina cold event. The surface heat budgets and sea surface temperature (SST) tendency for these two events in the tropical western Pacific and eastern Indian Oceans are investigated using the Goddard Satellite-retrieved Surface Radiation Budget (GSSRB) and Goddard Satellite-based Surface Turbulent Fluxes, version 2 (GSSTF2). It is found that the relative changes of surface heat budgets and SST tendency of the two events are quite different between the tropical eastern Indian and western Pacific Oceans.

Keywords: Surface heat budgets, SST tendency, El Nino, La Nina

1. Introduction

The tropical western Pacific and eastern Indian Oceans are characterized by the highest sea surface temperature (SST), frequent heavy rainfall, strong atmospheric heating and weak mean winds with highly intermittent westerly wind bursts. The heating drives the global climate and plays the key role in the El Nino–Southern Oscillation (ENSO) and the Asian-Australian monsoon (Webster et al. 1998). In addition, small changes in the SST of the Pacific warm pool associated with the eastward shift of the warm pool during the ENSO events have been shown to affect the global climate (Palmer and Mansfield 1984). Thus, the Tropical Ocean Global Atmosphere (TOGA) Coupled Ocean-Atmosphere Response Experiment (COARE) was conducted with the aim to better understand various physical processes responsible for the SST variation in the Pacific warm pool (Webster and Lukas 1992; Godfrey et al. 1998). The 1997-98 is a strong El Nino warm event, while the 1998-99 is a moderate La Nina cold event. We have compared the surface heat budgets, SST and tendency, deep convection, surface wind and stress for these two events in the tropical western Pacific and eastern Indian Oceans using satellite-derived surface fluxes (Chou et al. 2004). We briefly present the results in this paper.

2. Data

The data used are $1^{\circ} \times 1^{\circ}$ latitude-longitude monthly mean SST, surface radiative and turbulent fluxes, outgoing longwave radiation (OLR), and 10-m wind speed for October 1997-September 2000 cover the domain 30°S-30°N, 90°E-170°W. The SST of the NCEP/NCAR reanalysis (Kalney et al. 1996) is used. Deep convection is inferred from the OLR of NOAA's polar-orbiting satellites.

The radiative fluxes are taken from the Goddard Satellite-retrieved Surface Radiation Budget (GSSRB), derived from Japan Geostationary Meteorological Satellite-5 radiances (Chou et al. 2001). The GSSRB covers the domain 40°S-40°N, 90°E-170°W for a period of October 1997-December 2000. The spatial resolution is 0.5° x 0.5° latitude -longitude with a temporal resolution of one day. It is archived at http://daac.gsfc.nasa.gov/CAMPAIGN_DOCS/hydrology/hd_gssrb.html. Daily downward solar radiation has a bias of 6.7 W m^{-2} and a standard deviation (sd) error of 28.4 W m^{-2}, compared to the measurements at the US Department of Energy's Atmospheric Radiation Measurement (ARM) site on Manus Island (2.1°S, 147.4°E). Compared to the surface measurements at the ARM Manus site, the daily downward surface longwave radiation of GSSRB has a bias of +2.3 W m^{-2} and a sd error of 6.6 W m^{-2}.

The turbulent fluxes are taken from the Goddard Satellite-based Surface Turbulent Fluxes, version 2 (GSSTF2; Chou et al. 2003). The GSSTF2 contains daily, monthly, and climatological means of turbulent fluxes and the input parameters used in the derivation of fluxes over global oceans. The GSSTF2 has a spatial resolution of 1° x 1° latitude-longitude and covers the period July 1987-December 2000. Daily turbulent fluxes are derived from the Special Sensor Microwave/Imager (SSM/I) inferred surface air humidity (Chou et al. 1997), SSM/I surface winds (Wentz 1997), SST and 2-m air temperature of NCEP/NCAR reanalysis, based on surface layer similarity theory (Chou et al. 2003). To include the salinity effect, the surface saturation specific humidity of saline water is set to be 98% of pure water at the same SST. The flux measurements of five field experiments conducted by research ships in the tropical and midlatitude oceans during 1992-99 have been used for the validation. Compared to those of ship measurements, daily latent heat fluxes have a negative bias of -2.6 W m^{-2}, and a sd error of 29.7 W m^{-2}; daily sensible heat fluxes have a positive bias of 7.0 W m^{-2} and a sd error of 6.2 W m^{-2}; and daily wind stresses have a positive bias of 0.005 N m^{-2} and a sd error of 0.019 N m^{-2}. The GSSTF2 is archived at http://daac.gsfc.nasa.gov/CAMPAIGN_DOCS/hydrology/hd_gsstf2.0.html.

3. Results

We first analyze the mean surface heat budgets for the 3yr period October 1997 to September 2000 over the domain 30°S-30°N, 90°E-170°W (Chou et al. 2004). It is found that the magnitude of solar heating (F_{SW}) is larger than that of evaporative cooling (F_{LH}) but the spatial variation of the latter is significantly larger than the former. The range of the annual-mean is 180-240 W m^{-2} for F_{SW} and 80-190 W m^{-2} for F_{LH}. As a result, the spatial variations of seasonal and interannual variability of the net surface heating (F_{NET}) are dominated by the variability of F_{LH}. We also find that seasonal variations of F_{NET} and the SST tendency (dT_S/dt) are significantly correlated in the region, except for the equatorial western Pacific. The high correlation is augmented by the high negative correlation between solar heating and evaporative cooling. In the equatorial western Pacific, winds are weak, the oceanic mixed layer is shallow, and the solar radiation penetrating through the mixed layer is significant. Therefore, the relation between F_{NET} and dT_S/dt is weak.

To understand the changes in SST and atmospheric circulation over the tropical Pacific and Indian Oceans, we analyze the 1997/98 El Nino-minus-1998/99 La Nina differences of SST, OLR, zonal wind stress and 10-m wind speed over a large domain of 30°S-30°N, 40°E-120°W for the boreal winter of October-March as shown in Fig. 1. We then analyze the El Nino-La Nina differences of F_{SW}, F_{LH}, F_{NET}, and dT_S/dt over a small region 30°S-30°N, 90°E-170°W for the same winter seasons as shown in Fig. 2.

Compared to the La Nina, the SST during the El Nino increases by ~2-5°C in the central and eastern equatorial Pacific and by ~1°C in the western equatorial Indian Ocean, but decreases by <1°C near the maritime continent (Fig. 1a). Correspondingly, the OLR decreases by 40-60 W m^{-2} and 20 W m^{-2}, respectively, in the central equatorial Pacific and the western equatorial Indian Ocean, but increases by 20-40 W m^{-2} in the maritime continent (Fig. 1b). This is an indication of shifting the convection center from the maritime continent eastward to the central equatorial Pacific and westward to the western equatorial Indian Ocean.

In the equatorial region during the El Nino, the zonal wind stress increases (more westerly as trade winds weaken) east of ~150°E but decreases (more easterly as trade winds strengthen) west of ~150°E (Fig. 1c). In the equatorial region, the changes in OLR and zonal wind stress indicate a weakened Walker circulation in both the Pacific and Indian Oceans during the El Nino.

During the El Nino the zonal wind stress increases in the subtropical regions of the South Indian Ocean and North Pacific, but decreases in the southwestern Pacific near the SPCZ. The latter is due to the northward shift of the SPCZ as indicated by the OLR change. The wind stress change in the southern tropical Indian Ocean is a result of the equatorward shift of trade-wind belts during the El Nino (Yu and Rienecker 2000). The wind stress change around the South China Sea is an indication of increased subtropical high during the El Nino, which is consistent with the OLR change there.

Compared to the La Nina, the surface wind speed generally decreases by ~1-2 m s^{-1} during the El Nino, except for the regions extending from the southern section of the South China Sea to the maritime continent and further to the SPCZ where cloudiness decreases (Fig. 1d).

The change of F_{NET} between 1997-98 El Nino and 1998-99 La Nina during the boreal winter is significantly larger in the tropical eastern Indian Ocean than in the tropical western Pacific (Fig. 2c). For the tropical eastern Indian Ocean, Figs. 1 and 2 show that reduced evaporative cooling arising from weakened winds during the El Nino is generally associated with enhanced solar heating due to reduced cloudiness, leading to an enhanced interannual variability of F_{NET}. For the tropical western Pacific, reduced evaporative cooling due to weakened winds is generally associated with reduced solar heating arising from increased cloudiness, and vice versa. Consequently, the interannual variability of F_{NET} is reduced.

The change in dT_S/dt is generally larger in the tropical eastern Indian Ocean than in the tropical western Pacific (Fig. 2d). The correlation between interannual variations of F_{NET} and dT_S/dt is very weak for both regions. This result for the equatorial Pacific is consistent with that of Wang and McPhaden (2001) who found that all terms in the heat balance of the oceanic mixed layer contributed to the SST variation in the equatorial Pacific during the 1997-98 El Nino and 1998-99 La Nina. The low correlation is most likely related to the interannual variability of ocean dynamics.

The change in the zonal wind stress (Fig. 1c) suggests some important interannual changes in ocean dynamics. Compared to the La Nina, the change of ocean dynamics during the El Nino may include an increase of upwelling (downwelling) in the eastern (western) equatorial Indian Ocean and an increase in the interhemispheric heat transport from the south to the north Indian Ocean due to increased easterly wind forcing (Webster et al 1999; Yu and Rienecker 2000; Loschnigg and Webster 2000). It may also include an increase in heat transport from the equatorial western pacific to the equatorial central Pacific and a decrease in the heat transport from the Pacific to Indian Ocean by Indonesian throughflow due to increased westerly wind forcing in the equatorial Pacific (Godfrey 1996; Lukas et al. 1996; Meyers 1996). In addition, the solar radiation penetration through the oceanic mixed layer in the weak wind regions of the equatorial warm pool may change due to the change in surface wind, as suggested by previous studies (e.g., Anderson et al. 1996; Sui et al. 1997; Godfrey et al. 1998; Chou et al. 2000). Thus, we suggest that interannual changes of the surface heating and ocean dynamics all play important roles in the interannual variation of SST in this climatically important region. More observational and modeling studies are needed to validate our conclusions.

4. References

Anderson, S. P., R. A. Weller, and R. B. Lukas, 1996: Surface buoyancy forcing and the mixed layer of the western Pacific warm pool: observations and 1D model results. J. Climate, 9, 3056-3085.

Chou, M.-D., P.-K. Chan, and M. M.-H. Yan, 2001: A sea surface radiation dataset for climate applications in the tropical western Pacific and South China Sea. J. Geophys. Res., 106, 7219-7228.

Chou, S.-H., C.-L. Shie, R. M. Atlas and J. Ardizzone, 1997: Air-sea fluxes retrieved from Special Sensor Microwave Imager data. J. Geophys. Res., 102, 12705-12726.

Chou, S.-H., W. Zhao, and M.-D. Chou, 2000: Surface heat budgets and sea surface temperature in the Pacific warm pool during TOGA COARE. J. Climate, 13, 634-649.

Chou, S.-H., E. Nelkin, J. Ardizzone, R. M. Atlas, and C.-L. Shie, 2003: Surface turbulent heat and momentum fluxes over global oceans based on the Goddard satellite retrievals, version 2 (GSSTF2). J. Climate, 16, 3256-3273.

Chou, S.-H., M.-D. Chou, P.-K. Chan, P.-H. Lin, and K.-H. Wang, 2004: Tropical warm pool surface heat budgets and temperature: Contrasts between 1997/98 El Nino and 1998/99 La Nina. J. Climate, in press.

Godfrey, J. S, 1996: The effect of the Indonesian throughflow on ocean circulation and heat exchange with the atmosphere: A review. J. Geophy. Res., 101, 12217-12237.

Godfrey, J. S., R. A. House Jr., R. H. Johnson, R. Lukas, J.-L. Redelsperger, A. Sumi, and R. Weller, 1998: Coupled Ocean-Atmosphere Response Experiment (COARE): An interim report. J. Geophy. Res., 103, 14395-14450.

Kalnay, E., and co-authors, 1996: The NCEP/NCAR 40-year reanalysis project. Bull. Amer. Meteor. Soc., 77, 437-471.

Loschnigg, J., and P. Webster, 2000: A coupled ocean-atmosphere system of sst modulationfor the Indian Ocean. J. Climate, 13, 3342-3360.

Lukas, R, T. Yamagata, and J. P. McCreary, 1996: Pacific low-latitude western boundary currents and the Indonesian throughflow. J. Geophy. Res., 101, 12209-12216.

Palmer, T. N., and D. A., Mansfield, 1984: Response of two atmospheric general circulation models to sea-surface temperature anomalies in the tropical east and west Pacific. Nature, 310, 483-485.

Sui, C.-H., X. Li, K.-M. Lau, and D. Adamac, 1997: Mutiscale air-sea interactions during TOGA COARE. Mon. Wea. Rev., 125, 448-462.

Wang W., and M. J. McPhaden, 2001: Surface layer temperature balance in the equatorial Pacific during the 1997-98 El Nino and 1998-99 La Nina. J. Climate, 14, 3393-3407.

Webster, P. J. and R. Lukas, 1992: TOGA COARE: The TOGA coupled ocean-atmosphere response experiment. Bull. Amer. Meteor. Soc., 73, 1377-1416.

Webster, P. J. , T. Palmer, M. Yanai, V. Magana, J. Shukla, R. A. Toma, and A. Yasunari, 1998: Monsoons: Processes, Predicability and the prospects for prediction. J. Geophys. Res., 103, (C7), 14451-14510.

Webster, P. J., A. Moore, J. Loschnigg, and R. Leben, 1999: Coupled ocean–atmosphere dynamics in the Indian Ocean during 1997-1998. Nature, 401, 356-360.

Wentz, F. J., 1997: A well calibrated ocean algorithm for SSM/I. J. Geophys. Res., 102, 8703-8718.

Yu, L., and M. Rienecker, 2000: Indian Ocean warming of 1997-98. J. Geophys. Res., 105, 16923-16939.

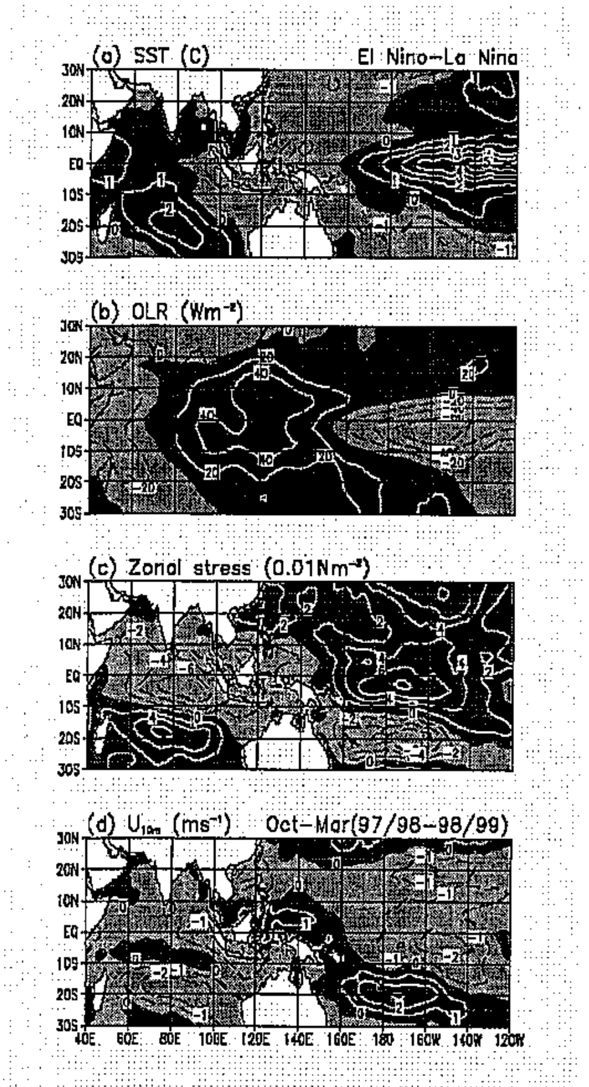

Fig. 1. 1997/98 El Nino-minus-1998/99 La Nina differences of (a) SST, (b) OLR, (c) zonal wind stress, and (d) 10-m wind speed for the boreal winter of October-March. Positive values are marked with dark shading, and negative values are marked with light shading.

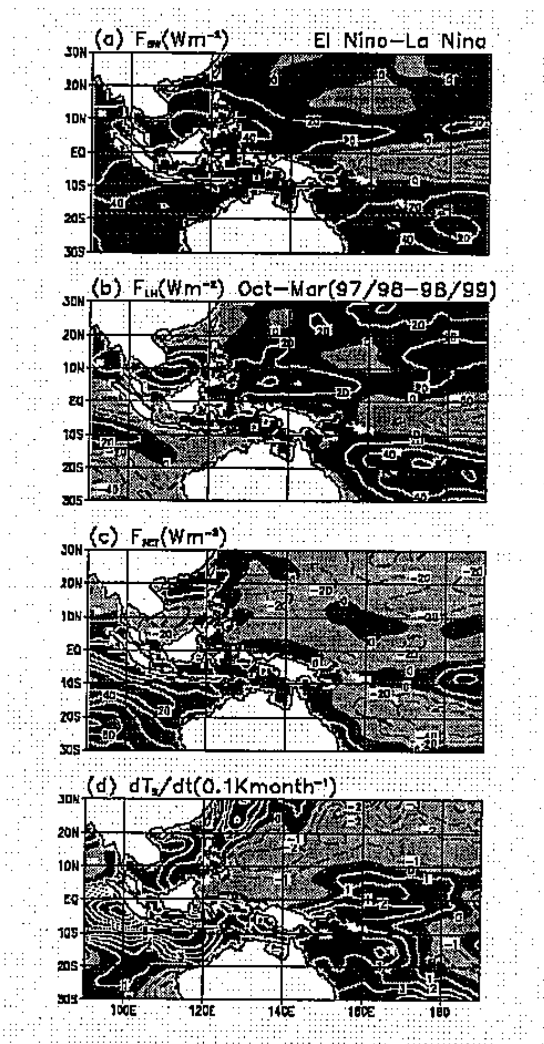

Fig. 2. As in Fig. 1, except for (a) solar heating, (b) evaporative cooling, (c) net surface heating, and (d) SST tendency.